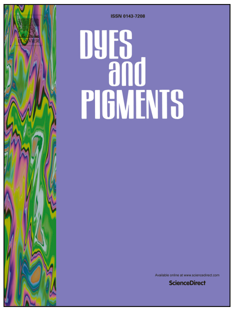

Preparation and Properties of Organo-soluble Tetraphenylethylene Monolayer-Protected Gold Nanorods

Tiantian Cao, Dengfeng Li, Xuyang Yao, Yikai Xu, Xiang Ma

PII: S0143-7208(15)00346-0

DOI: 10.1016/j.dyepig.2015.08.028

Reference: DYPI 4910

To appear in: *Dyes and Pigments*

Received Date: 25 June 2015

Revised Date: 28 August 2015

Accepted Date: 29 August 2015

Please cite this article as: Cao T, Li D, Yao X, Xu Y, Ma X, Preparation and Properties of Organo-soluble Tetraphenylethylene Monolayer-Protected Gold Nanorods, *Dyes and Pigments* (2015), doi: 10.1016/j.dyepig.2015.08.028.

Preparation and Properties of Organo-soluble Tetraphenylethylene Monolayer-Protected Gold Nanorods

Tiantian Cao, Dengfeng Li, Xuyang Yao, Yikai Xu and Xiang Ma*

Key Laboratory for Advanced Materials and Institute of Fine Chemicals, East China University of Science & Technology, Shanghai 200237, P. R. China

Tel: (+86) 21-6425-2288, Fax: (+86) 21-6425-2288, E-mail: maxiang@ecust.edu.cn

Graphical abstract

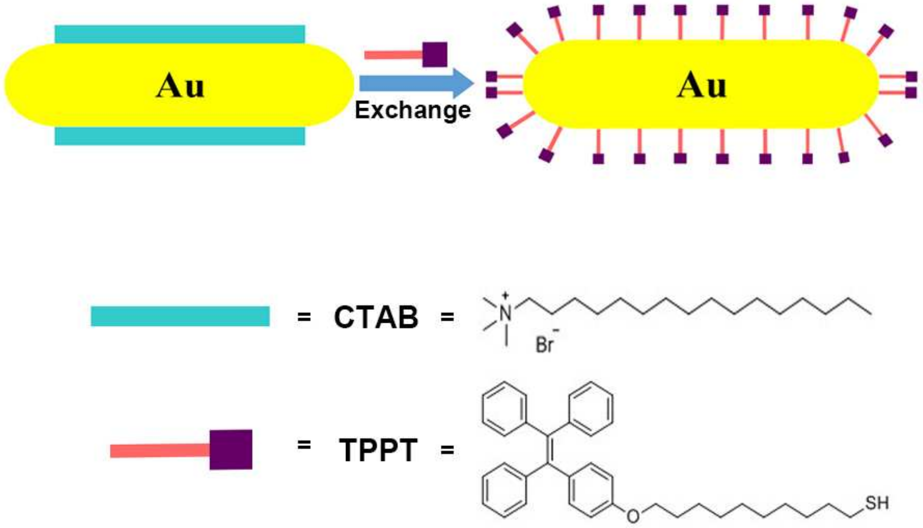

Preparation and Properties of Organo-soluble Tetraphenylethylene Monolayer-Protected Gold Nanorods

Tiantian Cao, Dengfeng Li, Xuyang Yao, Yikai Xu and Xiang Ma*

Key Laboratory for Advanced Materials and Institute of Fine Chemicals, East China University of Science & Technology, Shanghai 200237, P. R. China

Tel: (+86) 21-6425-2288, Fax: (+86) 21-6425-2288, E-mail: maxiang@ecust.edu.cn

Abstract

Organo-soluble tetraphenylethylene derived monolayer-protected gold nanorods were prepared and characterized. The prepared gold nanorods covered with tetraphenylethylene thiol via the strong covalent Au-S linkage were found to be soluble and stable in organic solvents. The successful thiol exchange and modification of tetraphenylethylene derivative molecules on gold nanorods were confirmed from UV-Vis, Raman and FT-IR spectra. The gold nanorods were found to have a quenching effect on the aggregation-induced emission of the tetraphenylethylene thiol molecule modified on their surfaces.

Keywords: Gold nanorod; Tetraphenylethylene; Monolayer; Aggregation-induced emission (AIE); Hybrid

1. Introduction

Nowadays, gold nanorods (**GNRs**) have attracted wide attention due to their anisotropic property and distinguishing surface plasmon resonance (**SPR**) [1-11]. **GNRs** usually have more distinguished physical properties particularly for their tunable absorption in the visible and near IR region, which are quite different from the widely investigated spherical gold nanoparticles (**GNPs**) [12]. **GNPs** have many promising applications in the areas of optics [13-15], sensors [16-18], biological imaging [19-21] and anticancer agents [22, 23]. Until now, **GNRs** have mainly been prepared in aqueous medium via the seed-mediated growth method [24-26], in which a surfactant cetyltrimethylammonium bromide (**CTAB**) was used as a shape-directing surfactant along their longitudinal axis to form a bilayer **CTAB** structure around the sidewall of **GNRs** and with their two ends free from **CTAB**. The resultant **GNRs** are water-soluble due to the protection of the surfactant **CTAB**. However, the **GNRs** protected by the bilayer **CTAB** structure are not very stable due to the fact that the dynamic **CTAB** layers can leave the **GNR** surface and result in the irreversible aggregation of **GNRs** into gold clusters. In addition, the **CTAB** molecules are toxic to proteins, tissues and biological cells, which limits their potential applications. It is well established that thiol molecules can form strong covalent S-Au bonds with the surface of **GNRs** and the resultant **GNRs** may readily disperse in organic solvents, which would provide a superior method to tune the properties of **GNRs** and enrich the application of **GNRs**. So far, only a few examples of thiol monolayer-protected **GNRs** have been reported because the preparation of thiol-monolayer-protected

GNRs was challenging [27-30].

Monolayer protected **GNRs** are fascinating hybrid materials composed of **GNRs** protected by an organic molecule monolayer, which solves the problem limited by the **CTAB** protecting layers. Great interest in the research in the **GNR** field continues to be drawn to focus on building **GNRs** protected by functional organic molecules. It is well known that modifying the chemical composition of **GNR** surfaces provides a versatile means to expand their various functions. In these cases, thiol molecules may exhibit superior stability compared with the **CTAB** molecules when they formed the strong covalent S-Au linkage with **GNRs**. Moreover, the thiol monolayer-protected **GNRs** may exhibit excellent solubility in organic solvents and distinguished surface functions [31-34]. However, it is noteworthy to point out that the exchange process of **CTAB** with lipophilic thiol molecules is not so easy since the **CTAB** molecules on the surface of **GNRs** are densely packed, which would make the thiol molecules difficult to access the gold surface to bind on the gold surface via a strong covalent Au-S linkage [28-32]. Not only that, the thiol molecules are attached onto the ends of **GNRs** primarily during the exchanging process [35, 36] since their two ends are free from **CTAB** and the thiol molecules would replace the lateral **CTAB** molecules with the extension of time. Without doubt, the preparation of these hybrid materials composed of **GNR** and organic molecules and tuning their properties would open the door to more fascinating applications of **GNRs** in the area of materials.

Aggregation-induced emission (**AIE**) is a rapidly growing, fascinating and challenging scientific area and has been intensively studied by Tang since 2001

[37-40]. Tetraphenylethylene (**TPE**) derivatives with their notable **AIE** performance have many applications [41-47]. In this work, a **TPE** derivatives containing compound 10-(4-(1,2,2-triphenylvinyl)phenoxy)decane-1-thiol (**TPPT**) was synthesized through a series of chemical reactions including McMurry reaction, Williamson reaction and hydrolysis reaction. **TPPT** was used to protect the entire surface of Gold nanorod via strong covalent S-Au bond for the first time (Fig. 1). The prepared **GNR** hybrids were stable in the organic solvent such as tetrahydrofuran (**THF**) without aggregation or decomposition and the successful modification on the surface of Gold nanorods was demonstrated via UV-Vis, Raman and FT-IR spectra. The gold nanorods were found to exhibit a quenching effect on the **AIE** fluorescence emission of the **TPPT** molecule modified on their surfaces.

Fig. 1 Schematic preparation of **TPPT** monolayer protected gold nanorods (**TGNRs**).

Fig. 2 Synthesis route of compound **TPPT.**

2. Experimental

2.1 General information

Benzophenone, 4-hydroxybenzophenone, 1,10-dibromodecane, **CTAB** and all the solvents were commercial available and used without further purification. ^{1}H and ^{13}C NMR spectra were measured on a Brüker AV-400 spectrometer. The electrospray ionization (ESI) high-resolution mass spectra were tested on a HP 5958 mass spectrometer. The UV-Vis absorption spectra were obtained on a Varian Cary 100 spectrometer (1-cm quartz cell was used). Transmission electron microscopy (TEM) experiments were done using JEOL JEM-2100 equipment. For the TEM observation, the samples in aqueous solution were dispersed on Cu grids pre-coated with thin carbon film (Cu-400 CN) and then completely dried for analysis. The FT-IR spectra were obtained on Nicolet 380 FT-IR spectrometer, the Raman spectra were carried out on inVia Reflex (Renishaw) spectrometer.

2.2 Synthesis and preparation

2.2.1 Synthesis of **TPPT** (Fig. 2)

4-(1,2,2-triphenylvinyl)phenol (**TPP**) was conveniently synthesized *via* a McMurry reaction in one step [43]. Zinc dust (2.18 g, 33.00 mmol), 4-hydroxy diphenyl ketone (1.65 g, 8.32 mmol), and benzophenone (1.50 g, 8.23 mmol) were added into a round-bottom flask in that order. The flask was then evacuated of air under vacuum and flushed with dry nitrogen several times. Anhydrous THF (80 mL) was then added into the flask, then the resultant mixture was cooled to 0 °C and $TiCl_4$ (1.88 mL, 16.50 mmol) was slowly added via syringe. The reaction proceeded at room temperature for half an hour, and then heated under refluxed for 8 h. K_2CO_3 solution (10 % aq.) was employed to quench the reaction and the solution extracted with diethyl ether several times. The organic layer was combined and washed with brine twice. The mixture was dried with anhydrous sodium sulfate and then the solvent was removed. The resulting residue was subjected to column chromatography using dichloromethane/petroleum ether (v/v 4:1) to give the 4-(1,2,2-triphenylvinyl)phenol

(1.40 g, 4.00 mmol, 50%, melting points: 225~226 °C). ^{1}H NMR (400 MHz, DMSO-d_6) δ 9.36 (s, 1H), 7.10 (ddd, J = 14.1 Hz, 11.7 Hz, 6.8 Hz, 9H), 6.95 (dd, J = 13.5 Hz, 7.3 Hz, 6H), 6.74 (d, J = 7.6 Hz, 2H), 6.50 (d, J = 7.6 Hz, 2H).

TPP (1.00 g, 2.87 mmol), 1,10-dibromodecane (4.31 g, 14.4 mmol) and potassium carbonate (0.59 g, 4.31 mmol) were added into a round-bottom flask, stirred and refluxed in CH_3CN (100 mL) under N_2 atmosphere for 12 h, then cooled to room temperature. The solution was filtered and the solvent was removed with rotavapor. Afterwards the crude product was purified on a silica-gel column using petroleum ether/dichloromethane (v/v 500:1) as eluent to yield (2-(4-((10-bromodecyl)oxy)phenyl)ethene-1,1,2-triyl)tribenzene (**BDTB**) as a white solid (0.98 g, 1.73 mmol, 60.1%, melting point: 58~62 °C). ^{1}H NMR (400 MHz, $CDCl_3$) δ 7.16 – 6.97 (m, 15H), 6.91 (d, J = 8.7 Hz, 2H), 6.62 (d, J = 8.7 Hz, 2H), 3.86 (t, J = 6.5 Hz, 2H), 3.41 (t, J = 6.9 Hz, 2 H), 1.91 – 1.80 (m, 2H), 1.78 – 1.66 (m, 2H), 1.42 (s, 4H), 1.30 (s, 8H). ^{13}C NMR (101 MHz, $CDCl_3$) δ 157.78 (s), 144.17 (d), 140.70 (s), 140.08 (s), 136.00 (s), 132.63 (s), 131.72 – 131.28 (m), 127.77 (d), 126.39 (d), 113.66 (s), 67.89 (s), 34.22 (s), 32.95 (s), 29.49 (t), 28.87 (s), 28.29 (s), 26.17 (s). TOF-MS (Fig. S4): $[M+H^+]^+$=567.2263, found 567.2263. FT-IR (Fig. S5): The asymmetrical stretching vibration of C-O-C was found at 1250 cm^{-1}. The signal at 1610 cm^{-1} of **BDTB** was attributed to the stretching vibration of benzene ring. The signals at 2926 cm^{-1} of CH_2 stretching vibration was observed in spectra.

BDTB (0.82 g, 1.44 mmol) and potassium ethanethioate (0.75 g, 6.53 mmol) were added to a flask containing CH_3CN (100 mL). And then the mixture was cooled to room temperature after stirred for 12 h under N_2 atmosphere. After the solvent being removed under vacuo, the crude product was extracted with ethyl acetate/H_2O and purified on a silica-gel column using petroleum ether/dichloromethane (v/v 20:1) as eluent to (10-(4-(1,2,2-triphenylvinyl)phenoxy)decyl)ethanethioate (**TPET**) as a white solid (0.524g, 0.931 mmol, 65%, melting point: 80~81 °C). ^{1}H NMR (400 MHz, $CDCl_3$) 7.14 – 6.98 (m, 15H), 6.91 (d, *J* = 8.6 Hz, 2H), 6.62 (d, *J* = 8.7 Hz, 2H), 3.86 (t, *J* = 6.5 Hz, 2H), 2.86 (t, *J* = 7.3 Hz, 2H), 2.32 (s, 3H), 1.77 – 1.66 (m, 2H), 1.28 (s, 14H). ^{13}C NMR (101 MHz, $CDCl_3$) δ 196.28 (s), 157.79 (s), 144.18 (d), 140.71 (s), 140.07 (s), 135.99 (s), 132.63 (s), 131.73 – 131.28 (m), 127.77 (d), 126.39 (d), 113.67 (s), 67.91 (s), 30.81 (s), 29.81 – 29.12 (m), 28.93 (s), 26.18 (s). TOF-MS (Fig. S8): $[M+Na^+]^+$=585.2798, found 585.2802. FT-IR (Fig. 4): The signals at 1652 cm^{-1} of **TPET** was attributed to the stretching vibration of -C=O-. The stretching vibration of benzene ring was found at 1635 cm^{-1}. The signal at 2921 cm^{-1} of CH_2 stretching vibration was observed in spectra.

TPET (0.25 g, 0.45 mmol), hydrazine monohydrochloride (0.12 g, 1.78 mmol) and sodium acetate (0.29 g, 3.55 mmol) were stirred together and refluxed in DMF (30 mL) for 12 h under N_2 atmosphere and then cooled to room temperature. After the solvent was removed under vacuo, the crude product was extracted with ethyl acetate/H_2O and purified on a silica-gel column using petroleum ether/dichloromethane (v/v 20:1) as eluent to yield compound **TPPT** (0.18 g, 0.346 mmol, 72%). ^{1}H NMR (400 MHz, $CDCl_3$) δ 7.12 – 6.98 (m, 15H), 6.91 (d, *J* = 8.7 Hz, 2H), 6.61 (d, *J* = 8.7 Hz, 2H), 3.86 (t, *J* = 6.5 Hz, 2H), 2.68 (t, *J* = 7.4 Hz, 2H), 1.77 –

1.62 (m, 4H), 1.44 – 1.25 (m, 13H).

2.2.2 Preparation of **CTAB-GNRs**

The **CTAB** bilayer coated **GNRs** were freshly prepared via the seed-mediated growth method [26]. The method can be divided into two steps. The preparation of gold seed is as following. 0.01 M solution of $HAuCl_4$ (0.250 mL) was added into 0.10 M **CTAB** solution (7.500 mL) in a vial. The solutions were gently mixed and the vial was lightly inverted several times. At this time, the solution showed bright brown-yellow. Then 0.01 M ice-cold $NaBH_4$ (0.600 mL) solution was added to the above solution all at once, followed by rapid inversion mixing for 2 min. Care should be taken to allow the produced gas escape in the mixing process. The solution appeared a pale brown-yellow color. Then the vial was kept in a water bath maintained at 25-30 °C for 2 hours. After that time, the seed solution was prepared and could be used for a week.

The preparation of **CTAB-GNRs** is as following. 0.10 M **CTAB** solution (9.500 mL) was added into an empty vial, then 0.01 M of $HAuCl_4$ (0.400 mL) and 0.01 M $AgNO_3$ (0.060 mL) solution were added into the vial one by one in that order. Then the solution was gently mixed by the inversion. The solution developed into bright brown-yellow. After that, 0.10 M AA solution (0.064 mL) was added into the above solution. Once the AA solution was added, the solution became colorless. In the end, seed solution (0.020 mL) was added, and mixed gently for 10 s. Then the vial was left undisturbed and kept in a water bath maintaining at 25-30 °C for 3 hours.

2.2.3 Synthesis of organic-soluble **TPPT** monolayer-protected **TGNRs**

At first, the solution of **CTAB** bilayer coated **GNRs** was centrifuged for 20 min at a speed of 12000 rpm for several times to remove the excessive **CTAB** and other impurities in the supernatant. Then the **CTAB-GNRs** were dispersed in ultrapure water (2 mL) and dispersed evenly by sonication. Next, the aqueous solution of **CTAB-GNRs** was added dropwise to a solution of 60 mg **TPPT** in THF (50 mL) with stirring under the protection of nitrogen. After that, the reaction flask was coated with silver paper and the color of the solution was purple. The reaction proceeded at room temperature for 48 hours. Then, the resultant **TGNRs** solution was centrifuged for 20 min at a speed of 12000 rpm three times to remove the excessive **CTAB** and the **TPPT** molecules. The resulting **TGNRs** were re-dispersed in THF (50 mL) with addition of excess **TPPT** and stirred for another 24 h. Similarly, the reaction proceeded under N_2 atmosphere and centrifuged for 20 min at a speed of 12000 rpm. The above procedure was repeated several times to ensure that the **GNRs** were well encapsulated with the **TPPT** molecules over the entire surface via the strong covalent S-Au bonds. At last, the mixture was centrifuged and washed with THF several times until there was no free **TPPT** molecules in the system of **TPPT** monolayer protected **TGNRs**, which could be confirmed from that there was no UV absorption band of **TPPT** molecule in the top layer solution. Then the **TPPT** monolayer protected **TGNRs** hybrid was successfully prepared. The resulting **TGNRs** can readily disperse in THF solution and without obvious aggregation, which was evidenced by transmission electron microscopy (TEM) observation (Fig. S10).

3. Results and discussion

3.1 Characterization of **TPPT** monolayer-protected **TGNRs**

The UV-Vis absorption spectra of **TPPT**, **GNRs** and **TGNRs** were employed to confirm the successful preparation of **TPPT** monolayer-protected **TGNRs**. Fig. 3 shows the two typical absorption peaks at 252 nm and 315 nm corresponding to **TPPT** and the two absorption peaks at 517 nm and 761 nm corresponding to the two **SPR** absorption bands of **GNRs**. After the **TPPT** monolayer protected **TGNRs** hybrid was successfully prepared, the two **SPR** absorption bands of **GNRs** had red-shifts by 54 nm and 39 nm to 571 nm and 800 nm, respectively.

Fig. 3 Absorption spectra of aqueous CTAB-**GNRs** (black), **TPPT** (red, 1.0 × 10^{-5} M) and **TGNRs** (blue).

The FT-IR spectrum of **TPET** was compared with that for **TGNRs** owing to the instability of thiol molecules (**TPPT**). The FT-IR spectra of **TPPT** monolayer protected **TGNRs** and **TPET** are shown in Fig. 4. The similar signals at 2921 cm^{-1} of CH$_2$ stretching vibration were observed in both spectra. The signals at 1435 cm^{-1} and 1506 cm^{-1} of **TGNRs** were attributed to the stretching vibration of a benzene ring. At the same time, benzene ring showed a characteristic out-of-plane bending vibration at 467 cm^{-1}. The signals at 1089 cm^{-1} of **TGNRs** were attributed to the asymmetrical stretching vibration of C-O-C. The FT-IR spectra also revealed the typical stretching vibration of C-S at 871 cm^{-1}. The comparison of **TGNRs** and **TPET** in the FT-IR spectra above helped to prove the successful modification of **TPPT** monolayer on the surface of **GNRs**.

Fig. 4 FT-IR spectra of **TPET** (blue) and **TGNRs** (red).

Fig. 5 Normalized Raman spectra of CTAB-**GNRs** (blue) and **TGNRs** (pink).

The successful modification of **TPPT** molecules on the surface of the GNRs via strong covalent S-Au linkages could also be evidenced from Raman spectroscopic data. As shown in Fig. 5, the Raman band of CTAB-**GNRs** at 162 cm^{-1} was attributed to Au-Br band. As expected, the characteristic Au-Br band disappeared in the Raman spectrum of the **TGNRs**, accompanied with the appearance of new Raman peaks especially corresponding to the Au-S band at around 126 cm^{-1} [30, 32]. The change of the spectra indicated that the existence of **TPPT** molecular monolayer around the surface of gold nanorods and no CTAB molecules remained on the surface of the **TGNRs**.

Fig. 6 Fluorescence intensity changes by gradually changing the ratio of THF and H_2O in the solution of (a) **TPPT** and (b) **TGNRs** (Excited at 310nm).

It is well known to all that the tetraphenylethylene (**TPE**) derivatives have a remarkable aggregation-induced emission (**AIE**) property. As seen in Fig. 6a, the fluorescence emission intensity of **TPPT** at 365 nm declined gradually when increasing the proportion of water in the solution of THF. While a new fluorescence emission band at 476 nm appeared when dissolving the **TPPT** in pure water. This was a typical AIE emission band of the **TPPB**, which was induced via a restricted intramolecular rotation (RIR) mechanism of **TPPT** molecules. Specifically, the hydrophobic **TPPT** molecule aggregated in water, restricting the rotation of the phenyl units of **TPPT** thus inducing the strong fluorescence emission with a red-shift by about 111nm [37-40]. The emission band of **TGNR** (Fig. 6b) at 365 nm corresponding to **TPPT** showed a blue-shift to 352 nm, as a result of the formation of **TGNR**. The same experimental methods were conducted to the **TGNR**, the fluorescence intensity of **TPPT** at 352 nm declined gradually when increasing the proportion of water in the solution of THF, which was similar with the situation of **TPPT**. The only difference was that there was no any obvious AIE fluorescence emission band in the range of longer wavelength of the fluorescence spectrum when dissolving the **TGNR** into the pure water, the reason of which might be that the **GNR** quenched the AIE (emission band at 476 nm) of **TPPT** fluorophore connected on its surface due to the electron transfer interaction from the Gold nanorods to the **TPPT** molecules very close on their surface [48].

4. Conclusion

In summary, we have successfully fabricated novel tetraphenylethylene (**TPE**) derivative monolayer-protected Gold nanorods **TGNRs** on the entire surface of **GNRs** via S-Au covalent linkages. The hybrid **TGNRs** were stable in organic solvents and without obvious aggregation. Besides, this hybrid showed quenching the AIE fluorescence emission of the tetraphenylethylene (**TPE**) derivatives. Construction of hybrid materials involving Gold nanorods remains challenging and employing these hybrid materials as smart materials are in progress.

Acknowledgments

This work is financially supported by NSFC (21421004, 21476075 and 21272072), and Shanghai Pujiang Program (13PJD011). T. Cao and D. Li contribute equally to this work.

References

[1] Bardhan R, Grady N K, Cole J R, Joshi A, Halas N J. Fluorescence enhancement by a nanostructures: nanoshells and nanorods. ACS Nano 2009; 3(3):744-752.

[2] Chen H, Shao L, Lia Q, Wang J. Gold nanorods and their plasmonic properties. Chem Soc Rev 2013; 42:2679-2724.

[3] Ni W, Yang Z, Chen H, Li L, Wang J. Coupling between molecular and plasmonic resonances in freestanding dye-gold nanorod hybrid nanostructures. J Am Chem Soc 2008; 130(21):6692-6693.

[4] Khalavka Y, Becke J, Sönnichsen C. Synthesis of rod-shaped gold nanorattles with improved plasmon sensitivity and catalytic activity. J Am Chem Soc 2009; 131:1871-1875.

[5] Fu Y, Zhang J, Lakowicz J R. Plasmon-enhanced fluorescence from single

fluorophores end-linked to gold nanorods. J Am Chem Soc 2010; 132(16):5540-5541.

[6] Ni W, Ambjornsson T, Apell SP, Chen H, Wang J. Observing plasmonic-molecular resonance coupling on single gold nanorods. Nano Lett 2010; 10(1):77-84.

[7] Ming T, Zhao L, Chen H, Woo K C, Wang J, Lin H Q. Experimental evidence of plasmophores: plasmon-directed polarized emission from gold nanorod-fluorophore hybrid nanostructures. Nano Lett 2011; 11(6):2296-2303.

[8] Li D X, Jang Y J, Lee J, Lee J E, Kochuveedua ST, Kim D H. Grafting poly(4-vinylpyridine) onto gold nanorods toward functional plasmonic coreeshell nanostructures. J Mater Chem 2011; 21:16453-16460.

[9] Sönnichsen C, Franzl T, Wilk T, von Plessen G, Feldmann J. Drastic reduction of plasmon damping in gold nanorods. Phys Rev Lett 2002; 88(7): 077402.

[10] Nikoobakht B, El-Sayed M A. Surface-enhanced raman scattering studies on aggregated gold nanorods. J Phys Chem A 2003; 107(18):3372-3378.

[11] Yao Y, Wang Y, Huang F. Synthesis of various supramolecular hybrid nanostructures based on pillar[6]arene modified gold nanoparticles/nanorods and their application in pH- and NIR-triggered controlled release. Chem Sci 2014; 5:4312-4316.

[12] Daniel M C, Astruc D. Gold nanoparticles: assembly, supramolecular chemistry, quantum-size-related properties, and applications toward biology, catalysis, and nanotechnology. Chem Rev 2004; 104: 293-346.

[13] Murphy C J, Sau T K, Gole A M, Orendorff C J, Gao J, Gou L, Hunyadi S E, Li

T. Anisotropic metal nanoparticles: synthesis, assembly, and optical applications. J Phys Chem B 2005; 109(29):13857-13870.

[14] Burda, C, Chen X B, Narayanan R, El-Sayed M A. Chemistry and properties of nanocrystals of different shapes. Chem Rev 2005; 105:1025−1102.

[15] Li H, Tan L L, Jia P, Li Q L, Sun Y L, Zhang J, Ning Y Q, Yu J, Yang Y W. Near-infrared light-responsive supramolecular nanovalve based on mesoporous silica-coated gold nanorods. Chem Sci 2014; 5: 2804-2808.

[16] Shigeyuki Y, Shingo N, Daisuke W, Hiroyuki N. Colorimetric sensing of metal ions by bis(spiropyran) podands: towards naked-eye detection of alkaline earth metal ions. Dyes Pigments 2009; 80:98-105.

[17] Yu C, Irudayaraj J. Multiplex biosensor using gold nanorods. Anal Chem 2006; 79(2):572-579.

[18] Sudeep P K, Joseph S T S, Thomas K G. Selective detection of cysteine and glutathione using gold nanorods. J Am Chem Soc 2005; 127(18):6516-6517.

[19] Huang X, El-Sayed I H, Qian W, El-Sayed M A. Cancer cell imaging and photothermal therapy in the near-infrared region by using gold nanorods. J Am Chem Soc 2006; 128(6):2115-2120.

[20] Pissuwan D, Valenzuela S M, Miller C M, Cortie M B. A golden bullet? selective targeting of toxoplasma gondii tachyzoites using antibody-functionalized gold nanorods. Nano Lett 2007; 7(12):3808-3812.

[21] Dreaden E C, Alkilany A M, Huang X, Murphy C J, El-Sayed M A. The golden age: gold nanoparticles for biomedicine. Chem Soc Rev 2012; 41:2740-2779.

[22] Chen C-C, Lin Y-P, Wang C-W, Tzeng H-C, Wu C-H, Chen Y-C, et al. DNA−gold nanorod conjugates for remote control of localized gene expression by near infrared irradiation. J Am Chem Soc 2006; 128(11):3709-3715.

[23] Tong L, Zhao Y, Huff T B, Hansen M N, Wei A, Cheng J X. Gold nanorods mediate tumor cell death by compromising membrane integrity. Adv Mater 2007; 19:3136-3141.

[24] Nikoobakht B, El-Sayed M A. Evidence for bilayer assembly of cationic surfactants on the surface of gold nanorods. Langmuir 2001; 17:6368-6374.

[25] Murphy C J, Jana N R. Controlling the aspect ratio of inorganic nanorods and nanowires. Adv Mater 2002; 14:80-82.

[26] Sau T K, Murphy C J. Seeded high yield synthesis of short Au nanorods in aqueous solution. Langmuir 2004; 20:6414-6420.

[27] Khanal B P, Zubarev E R. Rings of nanorods. Angew Chem Int Ed 2007; 46(13):2195-2198.

[28] El Khoury J M, Zhou X, Qu L, Dai L, Urbas A, Li Q. Organo-soluble photoresponsive azo thiol monolayer-protected gold nanorods. Chem Commun 2009; (16):2109-2111.

[29] Dai Q, Coutts J, Zou J, Huo Q. Surface modification of gold nanorods through a place exchange reaction inside an ionic exchange resin. Chem Commun 2008; (25):2858-2860.

[30] Li Y, Yu D, Dai L, Urbas A, Li Q. Organo-soluble chiral thiol-monolayer-protected gold nanorods. Langmuir 2011; 27(1):98-103.

[31] Xue C, Xu Y, Pang Y, Yu D, Dai L, Gao M, Urbas A, Li Q. Organo-soluble porphyrin mixed monolayer-protected gold nanorods with intercalated fullerenes. Langmuir 2012; 28(14):5956-5963.

[32] Cao J, Wu S, Zhai B, Wang Q, Li J, Ma X. Photo-responsive spiropyran monolayer protected gold nanorod. Dyes Pigm 2014; 103:89-94.

[33] Ma X, Xue Y, Dai L, Urbas A, Li Q. Hydrophilic cucurbit[7]uril pseudorotaxane anchored monolayer-protected gold nanorods. Eur. J. Inorg. Chem. 2013; 14:2082-2086.

[34] Ma X, Urbas A, Li Q. Controllable self-assembling of gold nanorods via On and Off supramolecular non-covalent interactions. Langmuir, 2012; 28(47):16263-16267.

[35] Caswell K K, Wilson J N, Bunz U H F, Murphy C J. Preferential end-to-end assembly of gold nanorods by biotin−streptavidin connectors. J Am Chem Soc 2003; 125(46):13914-13915.

[36] Yu C, Varghese L, Irudayaraj J. Surface modification of cetyltrimethylammonium bromide-capped gold nanorods to make molecular probes. Langmuir 2007; 23(17):9114-9119.

[37] Luo J, Xie Z, Lam J W Y, Cheng L, Chen H, Qiu C, Kwok H S, Zhan X, Liu Y, Zhu D, Tang B Z. Aggregation-induced emission of 1-methyl-1,2,3,4,5-pentaphenylsilole. Chem Commun 2001; (18):1740-1741.

[38] Hong Y, Lam JW, Tang B Z. Aggregation-induced emission: phenomenon, mechanism and applications. Chem Commun 2009; (29):4332-4353.

[39] Hong Y, Lam J W, Tang B Z. Aggregation-induced emission. Chem Soc Rev 2011; 40:5361–5388.

[40] Wang M, Zhang G, Zhang D, Zhu D, Tang B Z. Fluorescent bio/chemosensors based on silole and tetraphenylethene luminogens with aggregation-induced emission feature. J Mater C 2010; 20(10):1858-1867.

[41] Zhao Z, Deng C, Chen S, Lam J W, Qin W, Lu P, Wang Z, Kwok H S, Ma Y, Qiu H, Tang B Z. Full emission color tuning in luminogens constructed from tetraphenylethene, benzo-2,1,3-thiadiazole and thiophene building blocks. Chem Commun 2011; 47(31):8847-8849.

[42] Yu G, Tang G, Li Z, Yang J, Huang F. Supramolecular enhancement of aggregation-induced emission and its application in cancer cell imaging. J Mater Chem C 2014; 2:6609-6617.

[43] Yao X, Ma X, Tian H. Aggregation-induced emission encoding supramolecular polymers based on controllable sulfonatocalixarene recognition in aqueous solution. J Mater Chem C 2014; 2(26):5155-5160.

[44] Chen Z, Zhang J, Song M, Yin J, Yu G A, Liu S H. A novel fluorene-based aggregation-induced emission (AIE)-active gold(I) complex with crystallization-induced emission enhancement (CIEE) and reversible mechanochromism characteristics. Chem Commun 2015; 51: 326-329.

[45] Liu G, Liang J, Wu D, Li Z, Chen X, Liu S H, Yin J. Tetraphenylethene modified [n]rotaxanes: synthesis, characterization and aggregation-induced emission(AIE) behaviors. Org Biomol Chem 2015; 13: 4090-4100.

[46] Wang P, Yan X, Huang F. Host–guest complexation induced emission: a pillar[6]arene-based complex with intense fluorescence in dilute solution. Chem Commun 2014; 50:5017-5019.

[47] Yan X, Cook T R, Wang P, Huang F, Stang P J. Highly emissive platinum(II) metallacages. Nat Chem 2015; 7:342-348.

[48] Cannone F, Chirico G, Bizzarri A R, Cannistraro S. Quenching and Blinking of Fluorescence of a Single Dye Molecule Bound to Gold Nanoparticles. J Phys Chem B 2006; 110:16491−16498.

Figure Captions:

Fig. 1 Schematic preparation of **TPPT** monolayer protected gold nanorods (**TGNRs**).

Fig. 2 Synthesis route of compound **TPPT**.

Fig. 3 Absorption spectra of aqueous CTAB-**GNRs** (black), **TPPT** (red, 1.0×10^{-5} M) and **TGNRs** (blue).

Fig. 4 FT-IR spectra of **TPET** (blue) and **TGNRs** (red).

Fig. 5 Normalized Raman spectra of CTAB-**GNRs** (blue) and **TGNRs** (pink).

Fig. 6 Fluorescence intensity changes by gradually changing the ratio of THF and H_2O in the solution of (a) **TPPT** and (b) **TGNRs** (Excited at 310 nm).

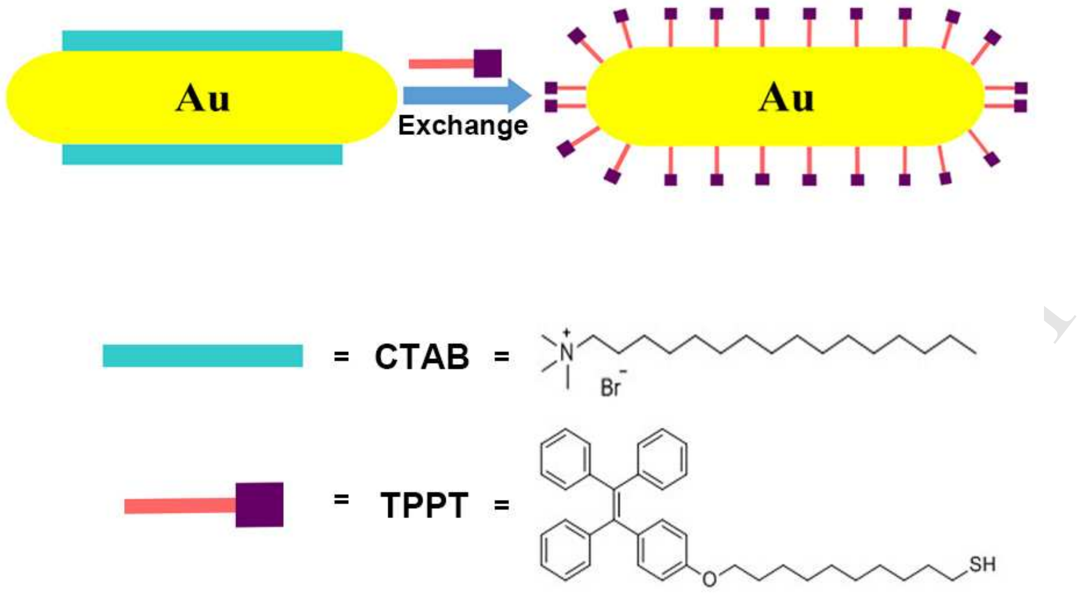

Fig. 1 Schematic preparation of **TPPT** monolayer protected gold nanorods (**TGNRs**).

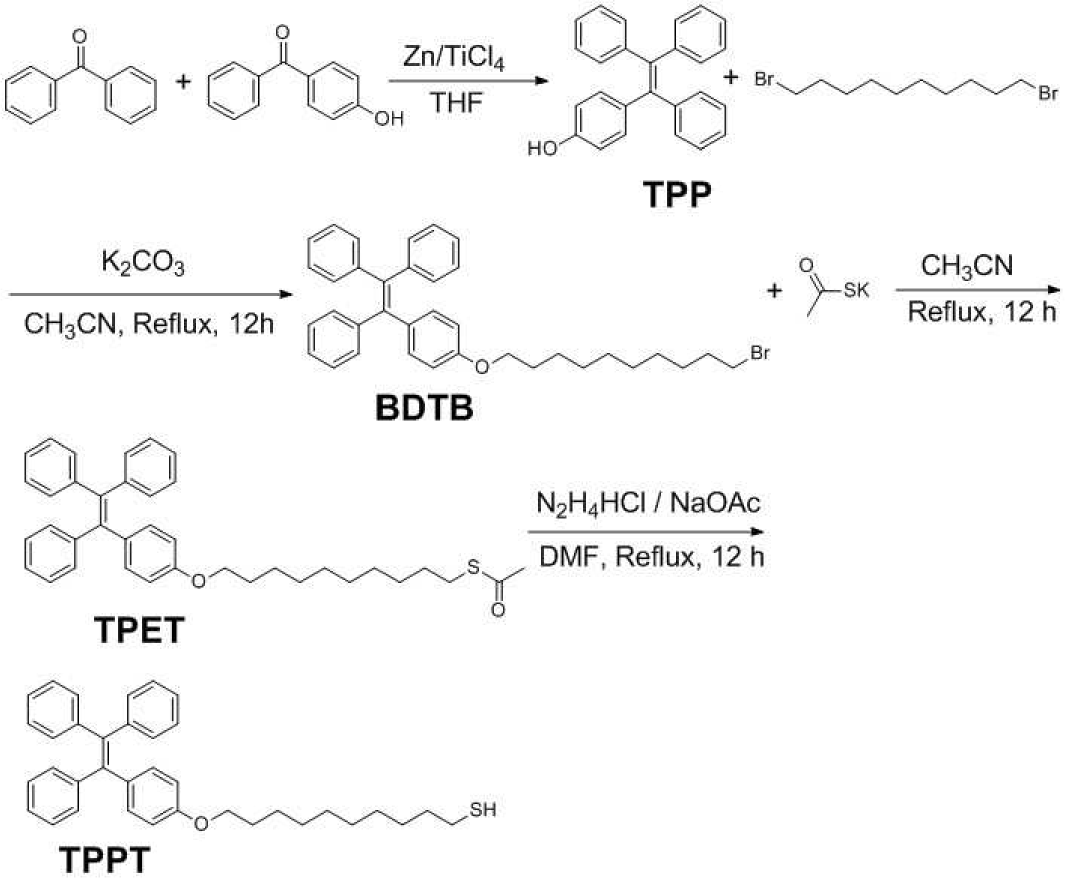

Fig. 2 Synthesis route of compound **TPPT**.

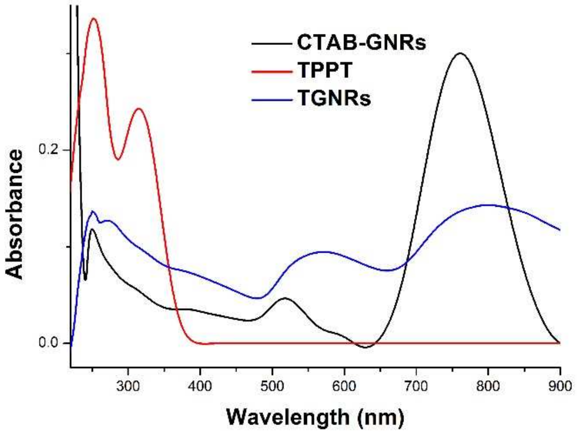

Fig. 3 Absorption spectra of aqueous CTAB-**GNRs** (black), **TPPT** (red, 1.0 × 10^{-5} M) and **TGNRs** (blue).

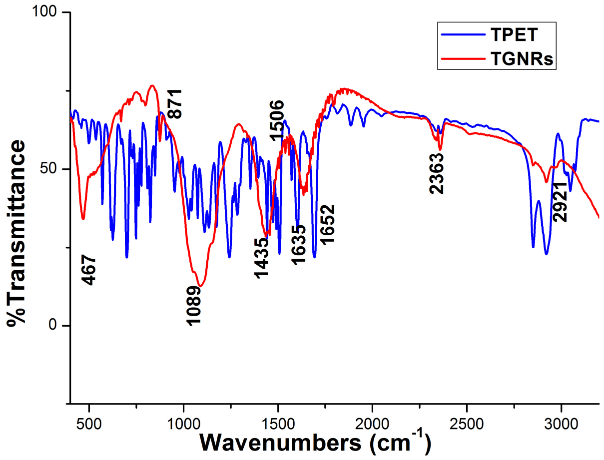

Fig. 4 FT-IR spectra of **TPET** (blue) and **TGNRs** (red).

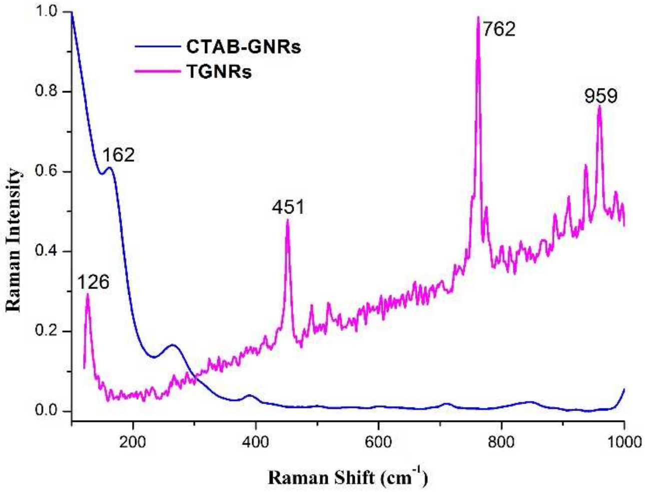

Fig. 5 Normalized Raman spectra of CTAB-**GNRs** (blue) and **TGNRs** (pink).

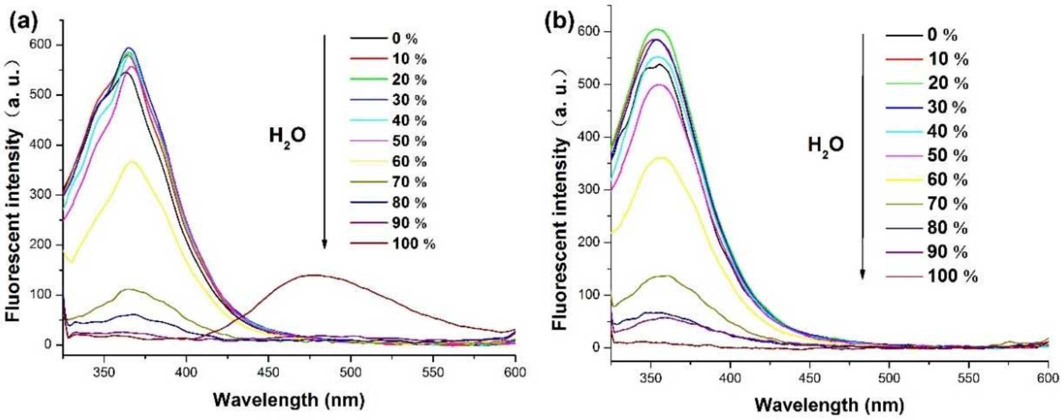

Fig. 6 Fluorescence intensity changes by gradually changing the ratio of THF and H_2O in the solution of (a) **TPPT** and (b) **TGNRs** (Excited at 310 nm).

Supplementary Information

Preparation and Properties of Organo-soluble Tetraphenylethylene Monolayer-Protected Gold Nanorods

Tiantian Cao, Dengfeng Li, Xuyang Yao, Yikai Xu and Xiang Ma*

Key Laboratory for Advanced Materials and Institute of Fine Chemicals, East China University of Science & Technology, Shanghai 200237, P. R. China

Tel: (+86) 21-6425-2288, Fax: (+86) 21-6425-2288, E-mail: maxiang@ecust.edu.cn

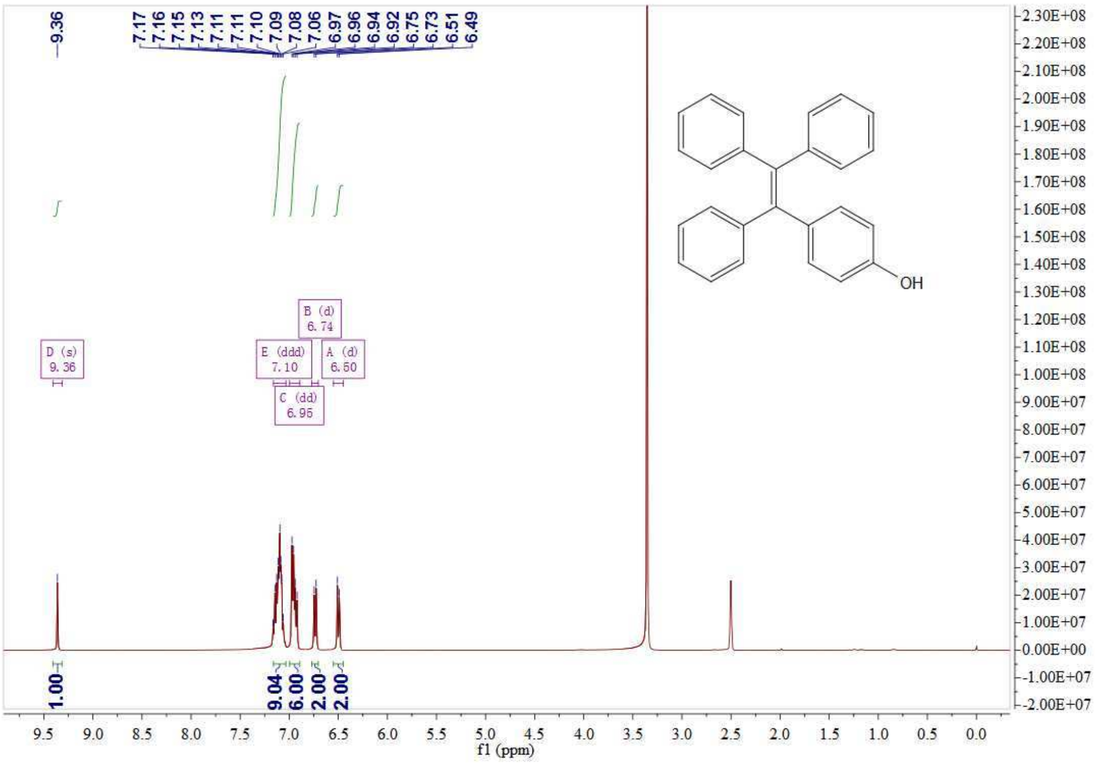

Fig. S1 ^{1}H NMR spectrum of **TPP** in DMSO-d_6.

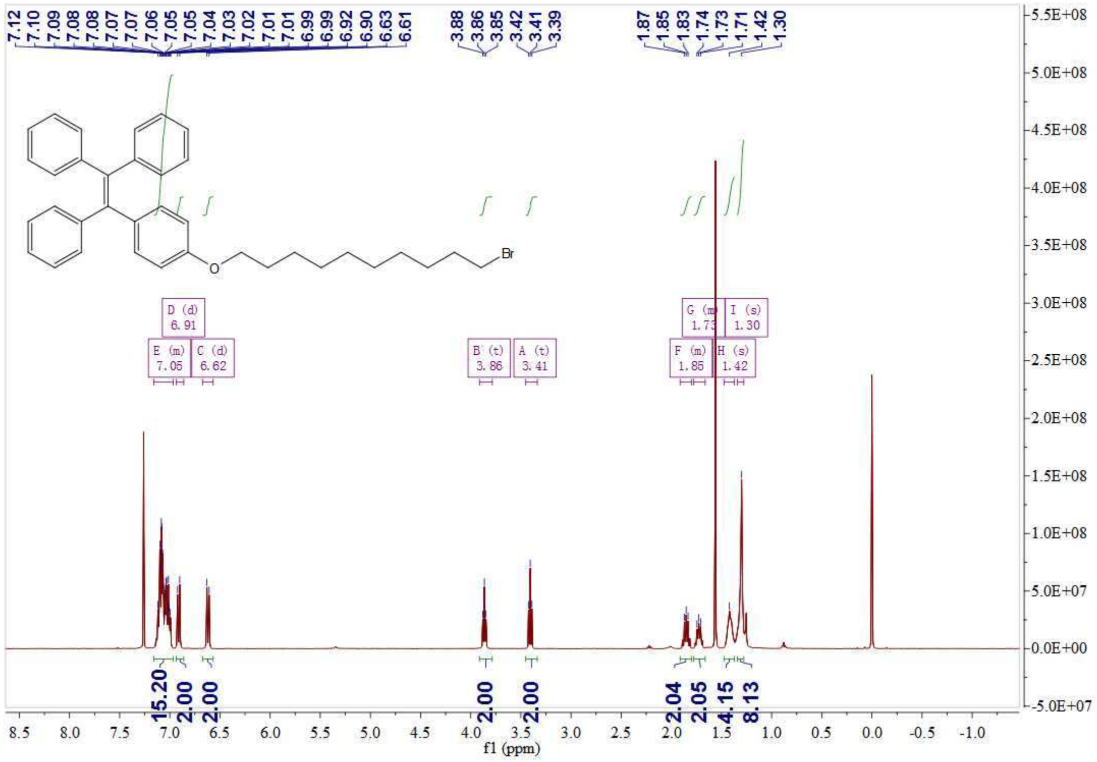

Fig. S2 ^{1}H NMR spectrum of **BDTB** in $CDCl_3$.

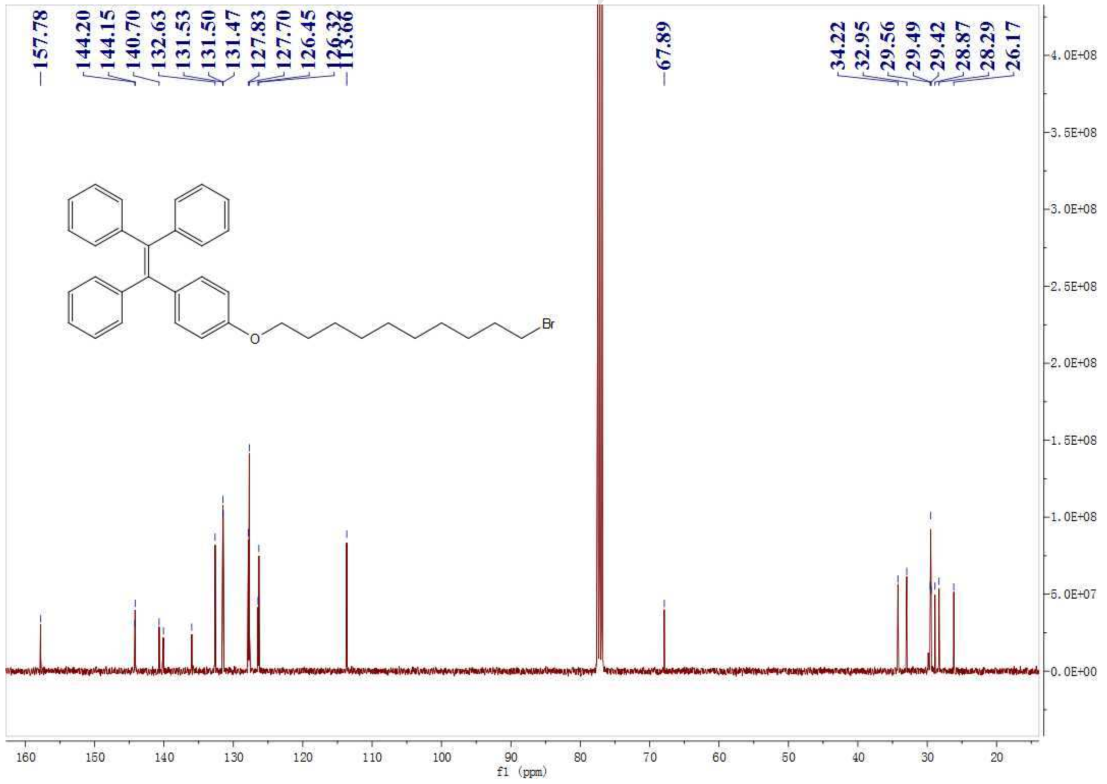

Fig. S3 ^{13}C NMR spectrum of **BDTB** in $CDCl_3$.

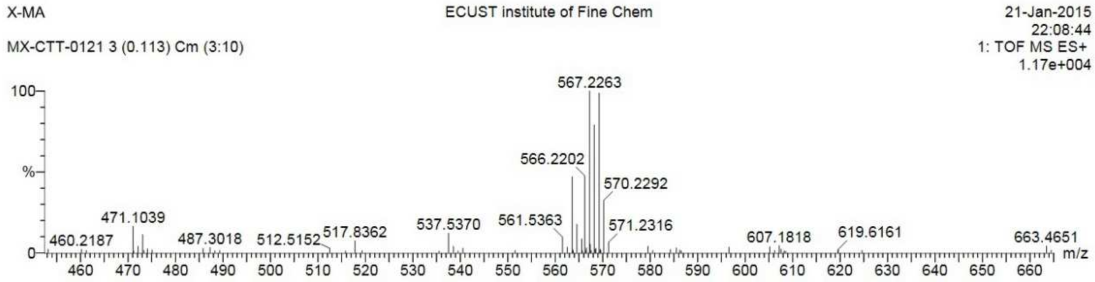

Fig. S4 TOF-MS of **BDTB**: [M+H$^+$]$^+$=567.2263, found 567.2263.

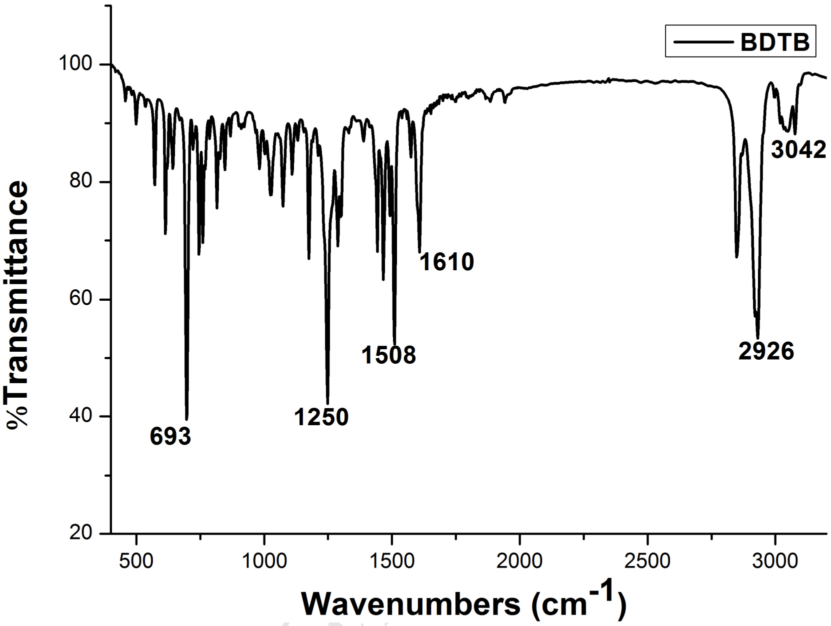

Fig. S5 FT-IR spectra of **BDTB**.

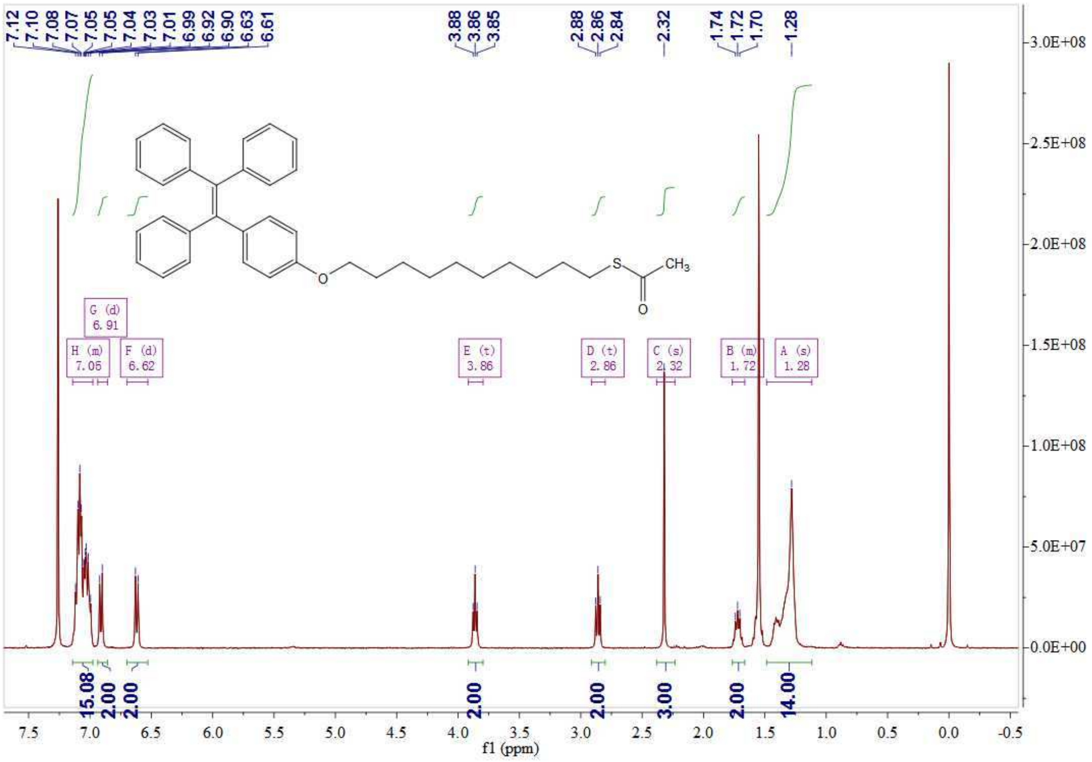

Fig. S6 ^{1}H NMR spectrum of **TPET** in CDCl$_3$.

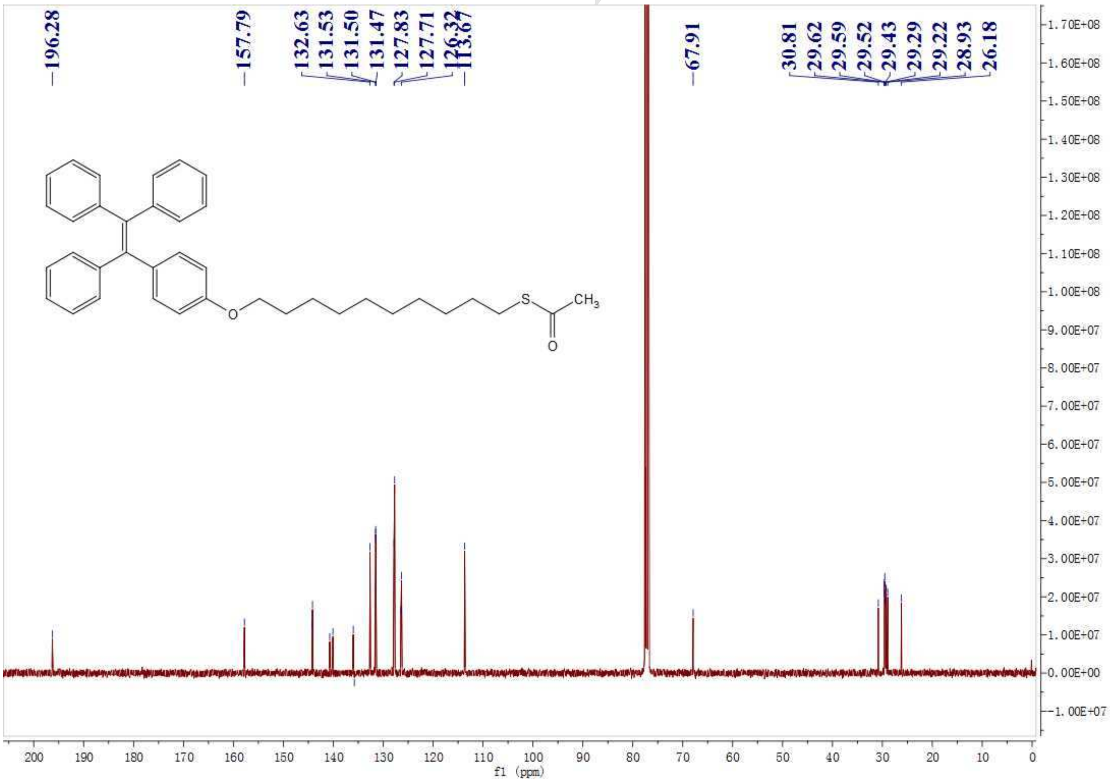

Fig. S7 ^{13}C NMR spectrum of **TPET** in CDCl$_3$.

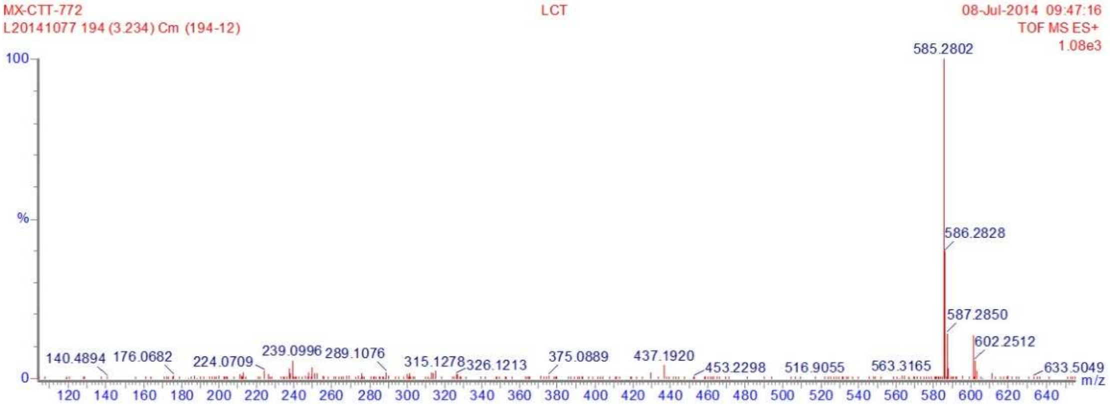

Fig. S8 TOF-MS of **TPET**: $[M+Na^+]^+$=585.2803, found 585.2802.

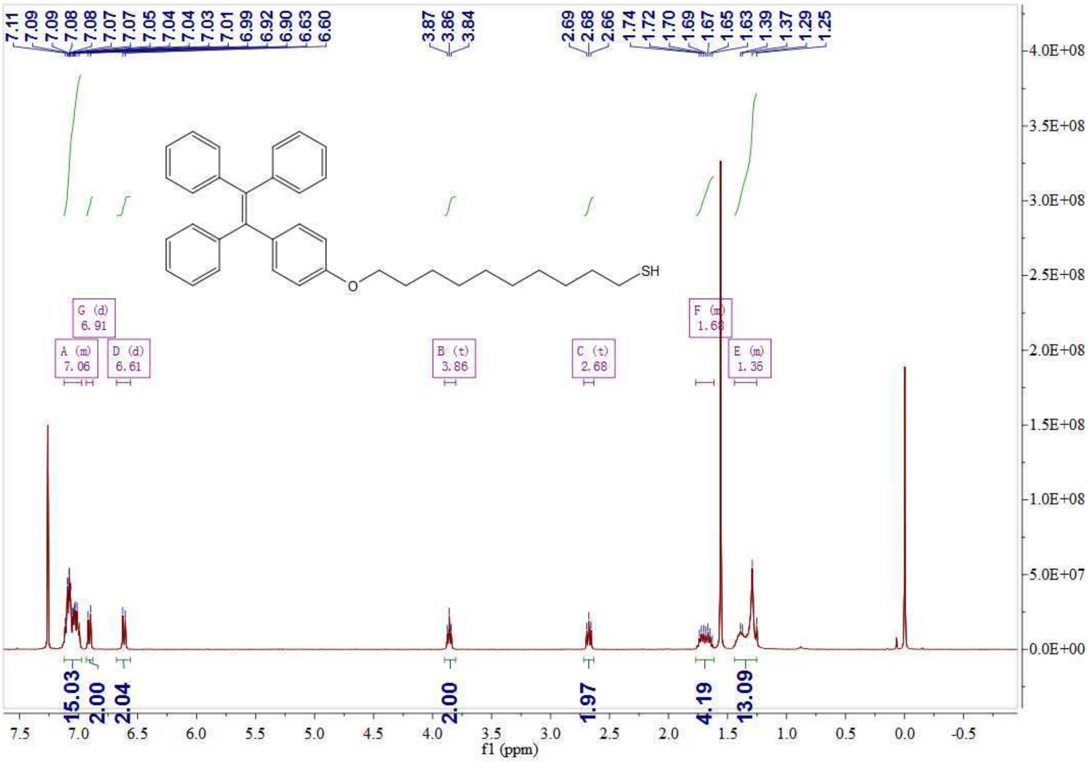

Fig. S9 ^{1}H NMR spectrum of compound **TPPT** in $CDCl_3$.

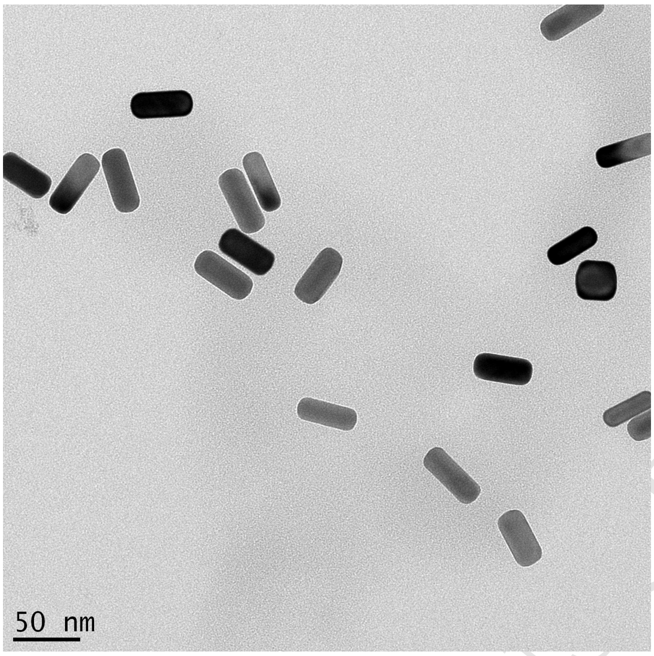

Fig. S10 TEM image of **TGNRs**.

Preparation and Properties of Organo-soluble Tetraphenylethylene Monolayer-Protected Gold Nanorods

Tiantian Cao, Dengfeng Li, Xuyang Yao, Yikai Xu and Xiang Ma*

Key Laboratory for Advanced Materials and Institute of Fine Chemicals, East China University of Science & Technology, Shanghai 200237, P. R. China

Tel: (+86) 21-6425-2288, Fax: (+86) 21-6425-2288, E-mail: maxiang@ecust.edu.cn

Highlights

1. Tetraphenylethylene monolayer protected Gold nanorod was successfully prepared.
2. Modification of Gold nanorod was confirmed by UV-Vis, Raman and FT-IR spectra.
3. Gold nanorods quenched the aggregation-induced emission of tetraphenylethylene.